Interaction of the phosphorylated DNA-binding domain in nuclear receptor CAR with its ligand-binding domain regulates CAR activation

Received for publication, July 13, 2017, and in revised form, November 10, 2017 Published, Papers in Press, November 13, 2017, DOI 10.1074/jbc.M117.806604

Ryota Shizu[‡], Jungki Min[§], Mack Sobhany[¶], Lars C. Pedersen[§], Shingo Mutoh[‡], and Masahiko Negishi[‡1]

From the Departments of [‡]Pharmacogenetics, Reproductive and Developmental Biology Laboratory, [§]Genome Integrity and Structural Biology Laboratory, and [¶]Nuclear Integrity, Signal Transduction Laboratory, NIEHS, National Institutes of Health, Research Triangle Park, North Carolina 27709

Edited by Joel Gottesfeld

The nuclear protein constitutive active/androstane receptor (CAR or NR1I3) regulates several liver functions such as drug and energy metabolism and cell growth or death, which are often involved in the development of diseases such as diabetes and hepatocellular carcinoma. CAR undergoes a conversion from inactive homodimers to active heterodimers with retinoid X receptor α (RXRα), and phosphorylation of the DNA-binding domain (DBD) at Thr-38 in CAR regulates this conversion. Here, we uncovered the molecular mechanism by which this phosphorylation regulates the intramolecular interaction between CAR's DBD and ligand-binding domain (LBD), enabling the homodimer–heterodimer conversion. Phosphomimetic substitution of Thr-38 with Asp increased co-immunoprecipitation of the CAR DBD with CAR LBD in Huh-7 cells. Isothermal titration calorimetry assays also revealed that recombinant CAR DBD-T38D, but not nonphosphorylated CAR DBD, bound the CAR LBD peptide. This DBD–LBD interaction masked CAR's dimer interface, preventing CAR homodimer formation. Of note, EGF signaling weakened the interaction of CAR DBD T38D with CAR LBD, converting CAR to the homodimer form. The DBD-T38D–LBD interaction also prevented CAR from forming a heterodimer with RXRα. However, this interaction opened up a CAR surface, allowing interaction with protein phosphatase 2A. Thr-38 dephosphorylation then dissociated the DBD–LBD interaction, allowing CAR heterodimer formation with RXRα. We conclude that the intramolecular interaction of phosphorylated DBD with the LBD enables CAR to adapt a transient monomer configuration that can be converted to either the inactive homodimer or the active heterodimer.

Nuclear receptor constitutive active/androstane receptor (CAR)[2] is activated either by endogenous stimuli such as growth and stress, or by exposures to exogenous chemicals including therapeutic drugs and environmental pollutants. Upon activation, CAR regulates various types of hepatic metabolism and cell signaling. Thus, CAR activation can become either a beneficial or a risk factor in developing various toxicities in response to drug/chemical exposures, drug–drug interactions, and diseases (*i.e.* diabetes, steatosis, cholestasis, and hepatocellular carcinoma) (1–6). In this regard, understanding the activation mechanism should help us to predict and prevent CAR-mediated adverse outcomes.

In transformed cells, CAR is a constitutively active nuclear receptor that spontaneously accumulates in cell nuclei, and forms a heterodimer with RXRα to activate target gene transcription. CAR represses this constitutive activity by phosphorylation of Thr-38 within the DNA-binding domain in both mouse and human primary hepatocytes and in mouse livers. Thus, the underlying mechanism that regulates CAR is phosphorylation and dephosphorylation of Thr-38 for inactivation and activation, respectively. Protein phosphatase PP2A and scaffold protein receptor for activated C kinase (RACK1) are key factors for dephosphorylation at Thr-38 (7). Epidermal growth factor (EGF) and insulin repress dephosphorylation at Thr-38 by activating their downstream kinase such as an extracellular signal-regulated kinase (ERK1/2) and dissociating PP2A/RACK1 from CAR (8, 9). This repression signal stimulates phosphorylated CAR to form a homodimer, which buries the binding motif for PP2A and RACK1, thereby evading dephosphorylation and retaining CAR in an inactive state in the cytoplasm (10). Phenobarbital (PB) antagonizes EGF and insulin by binding their receptors and inhibiting progression of their signals to induce dephosphorylation of CAR for its indirect activation (7, 9, 11). Moreover, monomerization of phosphorylated CAR initiates this dephosphorylation (10). On the other hand, CAR ligands such as 6-(4-chlorophenyl)imidazo[2,1-b][1,3]thiazole-5-carbaldehyde *O*-3,4-dichlorobenzyl)oxime (CITCO) directly bind phosphorylated CAR, which dissociates from ERK1/2, monomerizing CAR for dephosphorylation and acti-

This work was supported by National Institutes of Health Intramural Research program Grants Z01ES1005-01 and ZIA ES102645. The authors declare that they have no conflicts of interest with the contents of this article. The content is solely the responsibility of the authors and does not necessarily represent the official views of the National Institutes of Health.

This article contains Fig. S1.

[1] To whom correspondence should be addressed. Tel.: 919-541-2404; Fax: 919-541-0696; E-mail: Negishi@niehs.nih.gov.

[2] The abbreviations used are: CAR, constitutive active/androstane receptor; DBD, DNA-binding domain; GR, glucocorticoid receptor; HNF4α, hepatocyte nuclear factor 4α; ITC, isothermal titration calorimetry; LBD, ligand-binding domain; PB, phenobarbital; PPAR, peroxisome proliferator-activated receptor; RACK1, receptor for activated C kinase 1; RXR, retinoid X receptor; XRS, xenochemical response signal; NTD, N-terminal domain; CITCO, 6-(4-chlorophenyl)imidazo[2,1-b][1,3]thiazole-5-carbaldehyde *O*-3,4-dichlorobenzyl)oxime; Ni-NTA, nickel-nitrilotriacetic acid.

vation (10). Although the cell signaling that regulates CAR and how drugs such as PB utilize it to activate CAR have now been delineated, the molecular mechanism by which CAR integrates this cell signaling at the protein level remains unexplored.

Here, we have investigated interactions between the DNA- and ligand-binding domains of CAR to probe the molecular basis by which CAR dephosphorylates at Thr-38 for activation of transcriptional enhancer functionality. Co-immunoprecipitation assays of tagged proteins in Huh-7 cells and isothermal titration calorimetry (ITC) assays with bacterially expressed recombinant proteins were employed to delineate the nature and regulation of these interactions. We present experimental data demonstrating that phosphorylation of Thr-38 regulates the CAR DBD's interaction with the LBD in response to EGF, and discuss the hypothesis that the DBD regulates CAR activation through homodimer-monomer conversion in a phosphorylation-dependent manner.

Results

Phosphorylation strengthens DBD binding to LBD

Interaction between the DBD and LBD was examined by co-immunoprecipitation assays. For this, either a GFP-tagged CAR DBD T38D or CAR DBD T38A mutant was ectopically co-expressed with FLAG-tagged CAR LBD in Huh-7 cells. Whole cell extracts were then prepared for subsequent immunoprecipitations. CAR DBD was precipitated by an anti-GFP antibody and the resultant precipitates were subjected to Western blot analysis using an anti-FLAG antibody (Fig. 1*A*). The CAR LBD was far more effectively co-precipitated with CAR DBD T38D than with CAR DBD T38A. Furthermore, ITC was performed to examine this DBD–LBD interaction using recombinant CAR proteins expressed in and purified from *Escherichia coli* cells. CAR DBD T38D bound CAR LBD with the dissociation constant (K_d) of 3.44 μM (Fig. 1*B*). On the other hand, no binding was detected between CAR LBD and CAR DBD WT. In both co-immunoprecipitation and ITC assays, phosphomimetic mutation of Thr-38 enhanced CAR DBD binding of CAR LBD. As shown in Fig. 1, FLAG-tagged CAR LBD and GFP-tagged CAR LBD were co-precipitated, suggesting that two CAR LBDs interacted to form a homodimer. However, this co-immunoprecipitation was greatly decreased in the presence of CAR DBD T38D in Huh-7 cells (Fig. 1*C, arrow* by LBD). This decrease reciprocated the dramatic increase in co-precipitation of LBD with DBD (Fig. 1*C, arrow* by DBD). Additional co-immunoprecipitation assays were performed to examine whether the EGF signal regulates CAR DBD T38D interaction with CAR LBD. EGF treatment effectively ablated co-immunoprecipitation of DBD with LBD (Fig. 2). The ability of CAR DBD T38D to limit CAR LBD homodimerization (Fig. 1*C*) combined with the ability of EGF to inhibit CAR DBD T38D interactions with CAR LBD suggests homodimerization of CAR is regulated in a signal-dependent manner by EGF. This finding became the impetus for the subsequent investigation.

DBD interacts with LBD through D-box

CAR DBD encompasses amino acid residues from 8 to 78, from which two deletion constructs (residues 8–41 and 42–63) were generated and tagged with GFP (Fig. 3*A*). Full-length or deletion constructs were co-expressed with FLAG-tagged CAR LBD in Huh-7 cells, from which whole cell extracts were prepared for immunoprecipitation assays using an anti-FLAG antibody. The 42–63 construct, but not the 8–41 construct, was co-precipitated with CAR LBD (Fig. 3*B*). The 42–63 residues include the motif called D-box, which constitutes five amino acids at the N terminus of second zinc finger. The D-box is known to regulate DBD dimerization and DNA binding, whereas it does not bind DNA (12–14). Subsequently, the D-box motif within the 42–63 construct was highlighted as a potential target of this DBD–LBD interaction. All these amino acids, PFAGS, were mutated to arginine within the context of the 42–63 construct. The resultant mutant was co-expressed with FLAG-tagged and GFP-tagged CAR LBDs in Huh-7 cells. This mutant was not co-precipitated with CAR LBD (Fig. 3*C, arrow* by DBD). However, FLAG-tagged CAR LBD and GFP-tagged CAR LBD were co-precipitated in the presence of this mutant (Fig. 3*C, arrow* by LBD). Thus, these results delineated the interaction site of DBD with LBD to the D-box motif.

LBD interacts with DBD through a loop

CAR LBD has been suggested to form a homodimer through three loops: loop 1 (residues 142–145), loop 2 (residues 210–218), and loop 3 (residues 301–307) (10). Because the DBD–LBD interaction inhibited CAR LBD to form a homodimer (Fig. 1*C*), it was expected that one of these loops interact with the DBD. Peptide competition assays were employed to examine this expectation. GFP-tagged DBD-(42–63) construct and FLAG-tagged LBD were co-immunoprecipitated in the presence or absence of one of these peptides. A glucocorticoid receptor α (GR) loop peptide was used as a negative control. Only peptide 3 effectively inhibited co-precipitation of LBD with DBD (Fig. 3*D*). To further support the role of loop 3 in this interaction, residues within the D-box and loop 3 were mutated to positively charged arginine and negatively charged aspartic acid, respectively, within the context of CAR T38D. We termed this resultant mutant T38D construct E-mutant (Fig. 3*E*). These mutations should have strengthened the interaction between the D-box and loop 3. E-mutant was tagged with FLAG or GFP and ectopically co-expressed in Huh-7 cells, and whole cell extracts were subjected to co-immunoprecipitation assays to examine their interactions. Similarly, FLAG-tagged and GFP-tagged CAR T38D were co-expressed and co-precipitated as a positive control. As expected, these tagged CAR T38D proteins increased their co-immunoprecipitation in response to EGF treatment. In contrast, T38D E-mutant was unable to respond to EGF treatment (Fig. 3*E*). Thus, these results supported the notion that D-box and loop 3 mediate the DBD–LBD interaction and inhibit homodimerization of CAR.

Hinge regulates DBD–LBD interaction

GFP-tagged CAR T38D and FLAG-tagged CAR T38D, which were co-expressed in Huh-7 cells, were co-immunoprecipitated in response to EGF treatment (Fig. 4*B*). Reciprocally, EGF decreased co-immunoprecipitation of FLAG-tagged CAR T38D with RACK1 (Fig. 4*C*). These observations confirmed that CAR T38D forms a homodimer in response to EGF signal

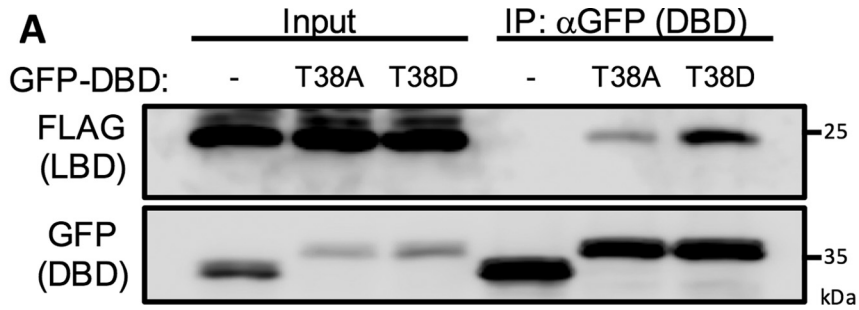

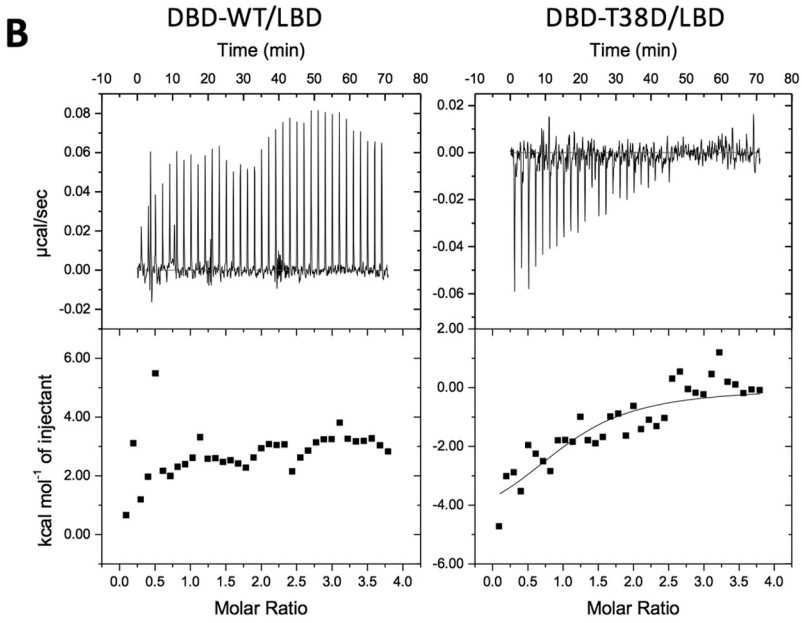

	DBD-WT/LBD	DBD-T38D/LBD
K_d (μM)	N.D.	3.44
ΔH (cal/mol)	N.D.	-5059±1568
ΔS (cal/mol/deg)	N.D.	7.67

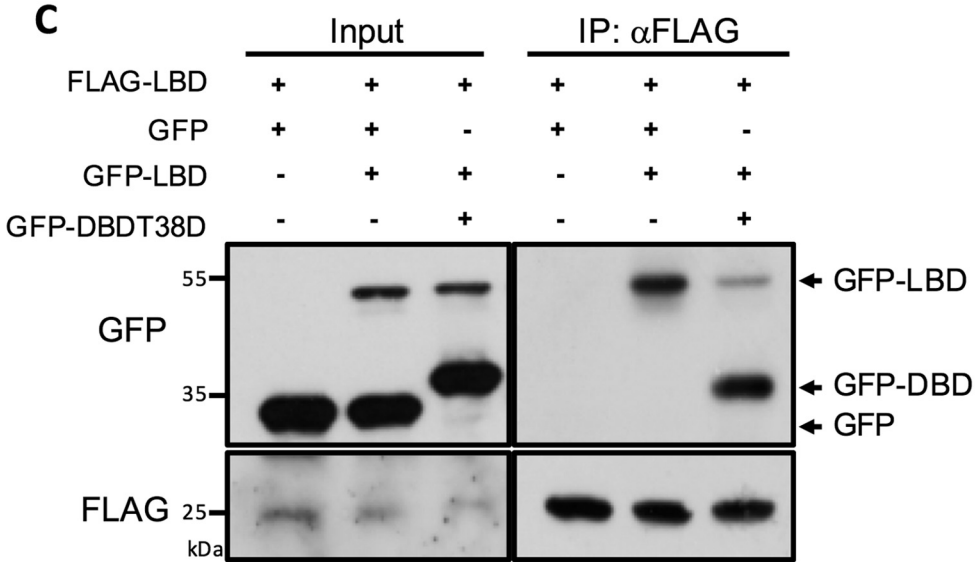

Figure 1. Regulation of the DBD–LBD interaction by phosphomimetic mutation of Thr-38. *A,* co-immunoprecipitation assays. FLAG–CAR–LBD and GFP–CAR–DBD T38A or T38D were co-expressed in Huh-7 cells from which whole extracts were prepared and immunoprecipitated with an anti-GFP antibody and analyzed by Western blots using given antibodies. *B,* ITC analysis. CAR–LBD (103–348) and CAR–DBD–WT or -T38D (7–87) (*K* (binding constant in M^{-1}), which is then converted to K_d (μM), Δ*H* (cal/mol), and Δ*S* (cal/mol/deg)]. *N.D.* means not detected. *C,* co-immunoprecipitation assays. FLAG–CAR–LBD and GFP–CAR–LBD were co-expressed with or without GFP–DBD–T38D in Huh-7 cells. Cell extracts were immunoprecipitated by an anti-FLAG antibody and analyzed by Western blots using the antibodies as shown.

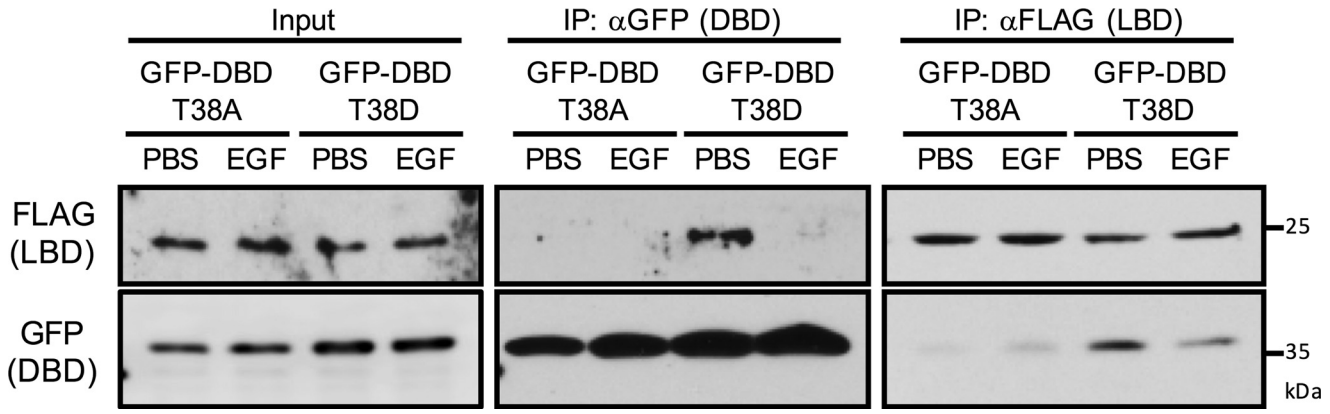

Figure 2. EGF regulation of the DBD–LBD interaction. Huh-7 cells co-expressing FLAG- and GFP-tagged CAR T38D were treated with 10 ng/ml of EGF for 30 min. Cell extracts were prepared and immunoprecipitated by an anti-FLAG or anti-GFP antibody for subsequent Western blots.

and dissociates RACK1 to evade dephosphorylation, as suggested by our previous findings (10). CAR T38DΔHinge (hereafter, ΔHinge) was generated by deleting hinge region residues 89 to 100 within the context of CAR T38D. FLAG-tagged ΔHinge was co-expressed with GFP-tagged CAR T38D in Huh-7 cells. Unlike CAR T38D, ΔHinge co-precipitated with CAR T38D in the absence of EGF treatment (Fig. 4*B*). Moreover, ΔHinge was not co-precipitated with RACK1 (Fig. 4*C*), and did not trans-activate a *CYP2B6* promoter in Huh-7 cell-based reporter assays even after CITCO treatment (Fig. 4*D*). Thus, the ΔHinge appeared to constitutively be maintained as a homodimer.

DBD regulates CAR–RXRα heterodimer

CAR is known to trans-activate gene promoters by forming a heterodimer with RXRα (15). Because phosphorylation at Thr-38 was found to abrogate CAR's DNA binding (11), we tested the hypothesis that this interaction also regulated heterodimerization with RXRα. FLAG-tagged CAR LBD and GFP-tagged RXRα LBD were co-expressed in the presence or absence of GFP-tagged CAR DBD T38D in Huh-7 cells. CAR and RXRα co-precipitated in the absence of CAR DBD T38D, but not in its presence (Fig. 5*A*, *arrow* by GFP RXR LBD). Under these conditions where heterodimerization was suppressed, CAR LBD increased its interaction with CAR DBD T38D (Fig. 5*A*, arrow by GFP DBD). To better understand how the CAR DBD regulates heterodimerization, three mutants were constructed using the CAR T38D construct to affect the interactions between the D-box of the DBD and loop 3 of the LBD, as shown in Fig. 5*C*. R-, E-, and S-mutants were designed to repel, tighten, and neutralize these interactions, respectively. Among them, the E-mutant can be expected to restrict the DBD binding to the LBD by enforcing the D-box–loop 3 interaction. Using these three mutants, *in vitro* pulldown assays were employed to examine their interactions with RXRα. The E-mutant was found not to pull down RXRα (Fig. 5*C*). Moreover, the E-mutant was unable to trans-activate a reporter gene in cell-based transfection assays (Fig. 5*D*). These studies suggest that the DBD–LBD interactions control regulation of CAR homodimerization and CAR heterodimerization with RXRα.

CAR T38D weakens DNA binding

CAR WT (residues 1–348) or its T38D mutant were expressed as SUMO conjugates in *E. coli* cells. After purification and removal of SUMO, these recombinant CARs were analyzed by size exclusion chromatography. Based on comparison to M_r standards, CAR WT preferentially eluted as a monomer, with about 10% being dimer (Fig. 6*A*). On the other hand, at least 50% of CAR T38D eluted as a dimer (Fig. 6*A*). The purity and content of the peaks was verified by SDS-PAGE (Fig. 6*B*) and mass spectrometry (data not shown). Utilizing these pure CAR constructs, fluorescence polarization was employed to examine binding of CAR to its enhancer DNA (DR4) from the *CYP2B6* promoter in the presence or absence of RXRα. Neither elicited polarization in the absence of RXRα. In the presence of RXRα, CAR WT bound DNA with the dissociation constant (K_d) of 169 ± 31 nM (Fig. 6*C*). CAR T38D exhibited weak binding with a K_d value of 1,231 ± 323 nM (Fig. 6*C*). These results suggest that phosphorylation of the DBD at Thr-38 not only regulates CAR homodimerization, but also heterodimerization with RXRα, thereby regulating the ability of CAR to bind DNA.

Discussion

CAR undergoes homodimer–heterodimer conversion to control its activity for regulatory activation. This conversion is regulated by phosphorylation of Thr-38 within the DBD. Phosphorylation strengthens an intramolecular interaction of the DBD with LBD, enabling phosphorylated CAR to be a monomer. Upon dephosphorylation of Thr-38 by PP2A and RACK1, the DBD dissociates from the LBD, allowing dephosphorylated CAR to form a heterodimer with RXRα for activation. Conversely, this phosphorylated CAR monomer can also be converted to a phosphorylated homodimer, suppressing its constitutive activity. This homodimerization is regulated by EGF signaling, which weakens the interaction of phosphorylated LBD with the DBD. Based on these observations of protein–protein interactions in solution, the regulatory process of CAR is schematically depicted in Fig. 7. The intramolecular DBD–LBD interaction is the underlying mechanism by which CAR regulates its conversions, and the phosphorylated CAR monomer is positioned such that it can be converted to an inactive homodimer or to an active heterodimer with RXRα. In our

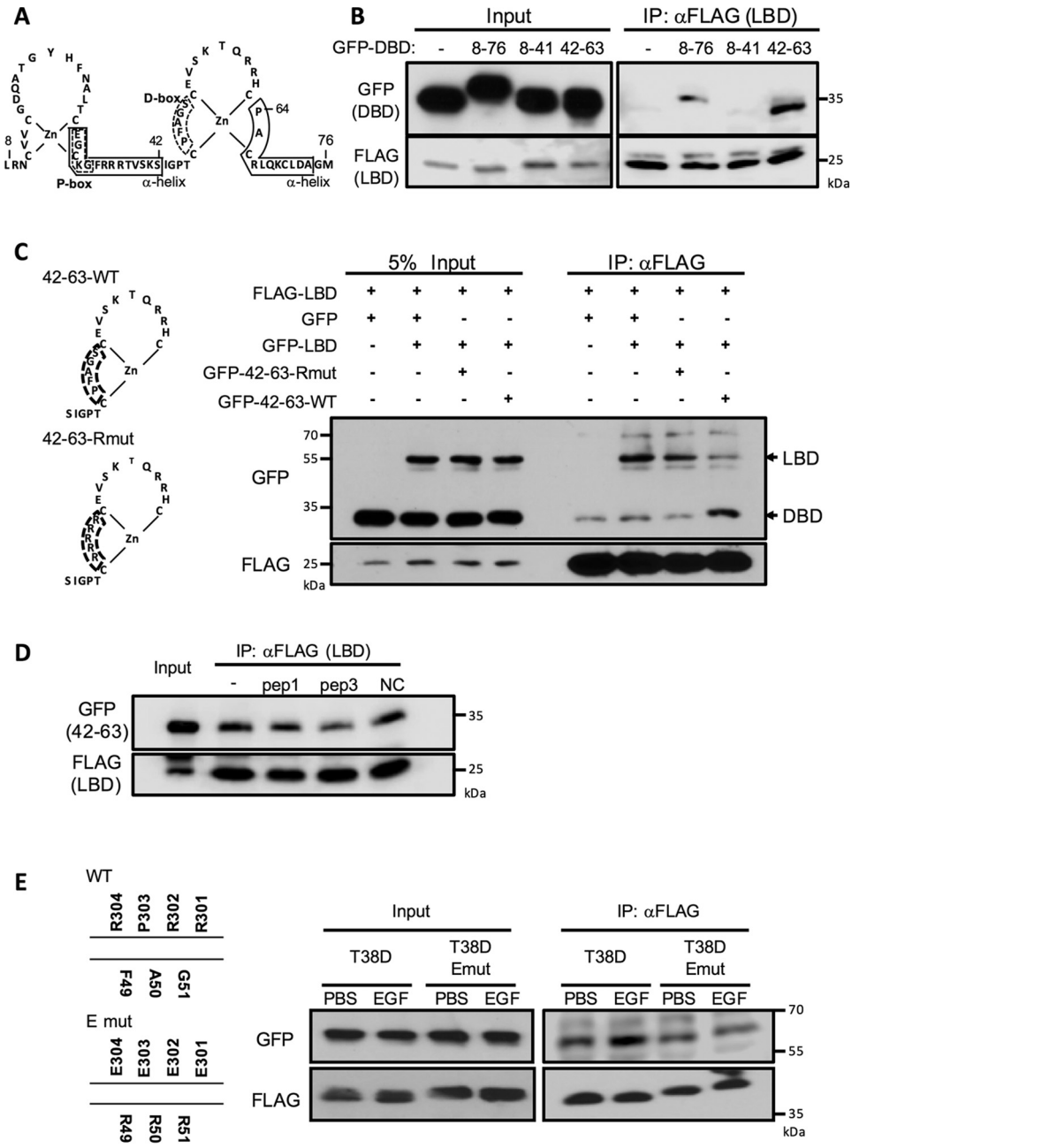

Figure 3. Characterization of the interface between DBD and LBD. *A,* map of the human CAR DBD. Single letter codes for amino acids are used. P-box and D-box are *circled by broken lines*. *B,* whole lysates from Huh-7 cells overexpressed with FLAG–CAR–LBD and GFP–CAR–DBD constructs (residues 8–76, 8–41, or 42–64) were subjected to co-immunoprecipitation by an anti-FLAG antibody or subsequent Western blots. *C,* FLAG–CAR–LBD and GFP–CAR–LBD were co-expressed in Huh-7 cells with GFP-CAR-DBD deletion mutant (residues 42–64) or GFP–CAR–DBD Rmut in which five amino acids within the D-box were mutated to arginine within the context of GFP–CAR–DBD deletion mutant (residues 42–64). The maps of the mutants are shown on the *left*. Cell extracts were subjected to a co-immunoprecipitation assay by an anti-FLAG antibody for subsequent Western blots. *D,* cell lysates from Huh-7 cells expressed with FLAG–CAR–LBD and GFP–CAR–DBD deletion mutants (residues 42–64) were incubated with LBD peptides (100 μM) and subjected to co-immunoprecipitation assay. Peptides 1 and 3 are residues 138–147, PAHLFIHHQP, and 299–308, QQRRPRDRFL of CAR, respectively. *NC* is one loop of GR (541–557; PEVLY-AGYDSSVPDSTW) as a negative control. *E,* Huh-7 cells were overexpressed with FLAG- and GFP-tagged CAR T38D or FLAG- and GFP-tagged CAR T38D-Emut and treated with EGF for 30 min. Cell lysates were subjected to co-immunoprecipitation assays with an anti-FLAG antibody. The amino acid sequences and E-mutations are depicted on the *left*. Band intensities of each data were quantified and are shown in Fig. S1.

previous studies, phosphorylation at Thr-38 was found to regulate CAR activation (*i.e.* nuclear translocation, DNA binding as a trans-activation) and confirmed in mouse livers as well as with mouse primary hepatocytes or *in vitro* binding assays (7, 10, 16). Given these findings, this phosphorylation-mediated interaction between the DBD and LBD should also be the molecular basis for endogenous CAR activation in an *in vivo* set up.

Our model of CAR dimerization conversions supports a role of the hinge to create separation between the DBD and LBD such that these two domains are not interacting in an inactive homodimer (Fig. 7*A*). In this model, the hinge acts as a spring connecting the DBD and LBD to regulate their interactions. CAR would then stretch this spring to form its homodimer or bend it to remain a monomer. When the hinge was deleted,

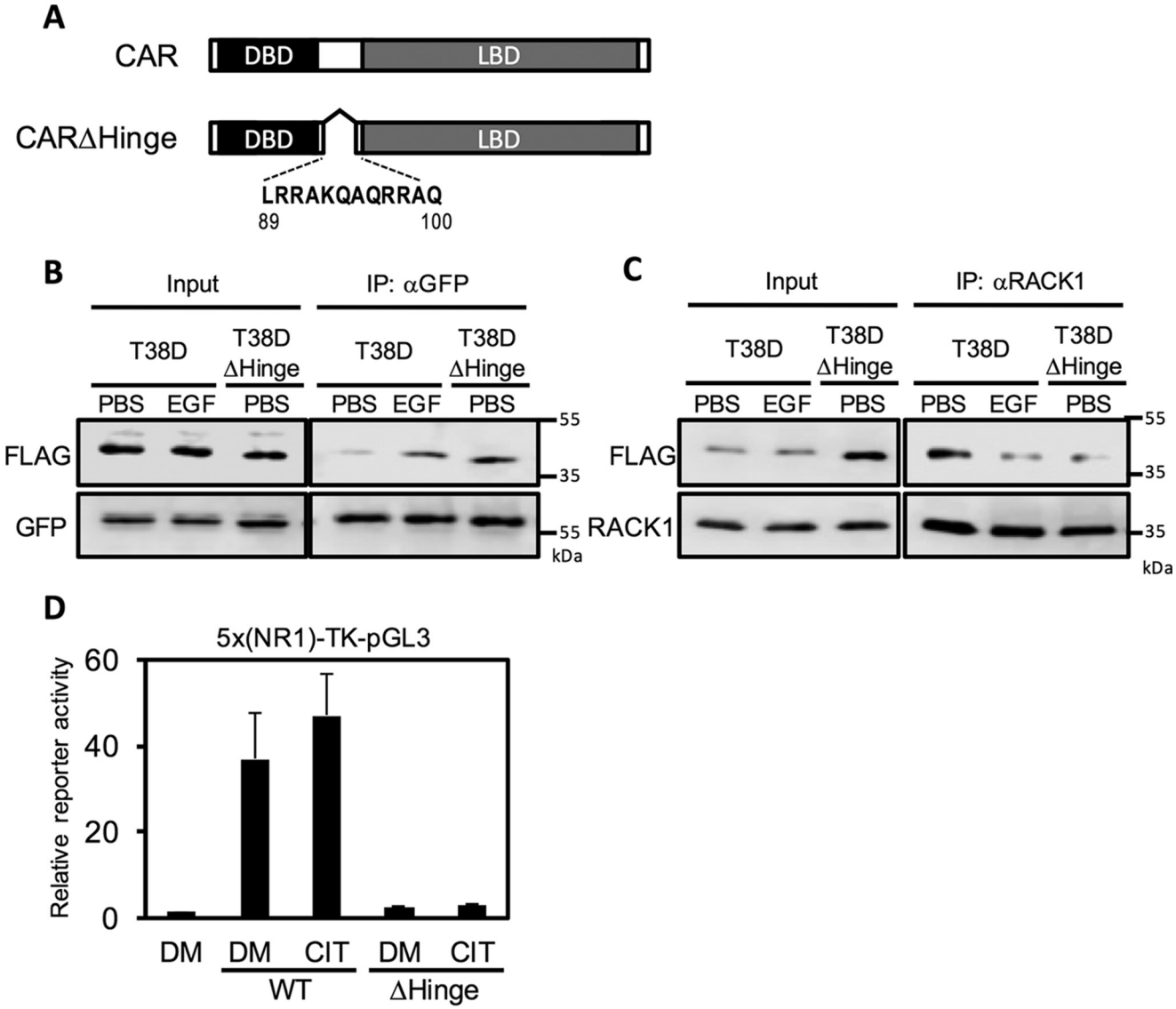

Figure 4. Regulation by the hinge region of the DBD–LBD interaction. *A,* the map of human CAR and CAR ΔHinge in which residues from 89 to 100 were deleted. *B* and *C,* Huh-7 cells were overexpressed with FLAG- and GFP-tagged CAR T38D and CAR T38DΔHinge, and treated with 10 ng/ml of EGF for 30 min. Cell lysates were subjected to a co-immunoprecipitation assay by anti-GFP antibody (*B*) or by anti-RACK1 antibody (*C*) for subsequent Western blots. *D,* Luc-reporter assays. Huh-7 cells were transfected with 5x(NR1)-TK-pGL3, phRL-TK, and expression plasmids for wild-type CAR or CAR ΔHinge and were treated with 0.1% DMSO (*DM*) or CITCO (*CIT*, 1 μM) for 24 h. Reporter activities were measured. Values are the mean ± S.D. ($n = 4$).

CAR lost this flexibility to position the DBD relative to LBD and remained a homodimer, unable to convert to either a monomer or heterodimer (Fig. 4) and unable to translocate to nucleus (17). In contrast, deletion of the hinge region in GR and progesterone receptor inhibited homodimer formation (18, 19).

In the X-ray crystal structure of DNA-bound hepatocyte nuclear factor 4α (HNF4α), a homodimer is observed that utilizes helices 10 and 11 to form the dimer interface, which was located opposite from the surface that constitutes the CARs homodimer region without DNA present (CAR only binds DNA as an RXRα heterodimer). In this HNF4α homodimer, the DBD of one monomer is interacting with the LBD of the other monomer, in which, serine 78 of the DBD (corresponds to Thr-38 of CAR) interacts with the loop that corresponds to loop 3 of CAR. The authors suggested a scenario that phosphorylation of serine 78 disrupts this interaction, dissociating the intermolecular interaction between DBD and LBD and inactivating HNF4α. This scenario is different from our hypothesis of the CAR activation mechanism depicted in Fig. 7. In our present CAR studies, phosphorylation of Thr-38 strengthened the intra-molecular interaction between the D-box and loop 3 (Fig. 7, *B* and *C*). Thr-38 resides in the helix between the two zinc fingers. Our dynamic computer simulation study had previously suggested that phosphorylation of Thr-38 causes a conformational alteration from this helix toward the second finger where the D-box is located (11). Taking these simulations into consideration, phosphorylated Thr-38 may not necessarily interact with loop 3 directly, but phosphorylation-initiated conformational changes may help the D-box interact with loop 3, strengthening the DBD–LBD interaction. This would be consistent with our hypothesis that the DBD and LBD dissociate when CAR forms either an inactive homodimer or an active heterodimer with RXRα. This dissociation is also observed with thyroid hormone receptor that dissociates its DBD–LBD inter-

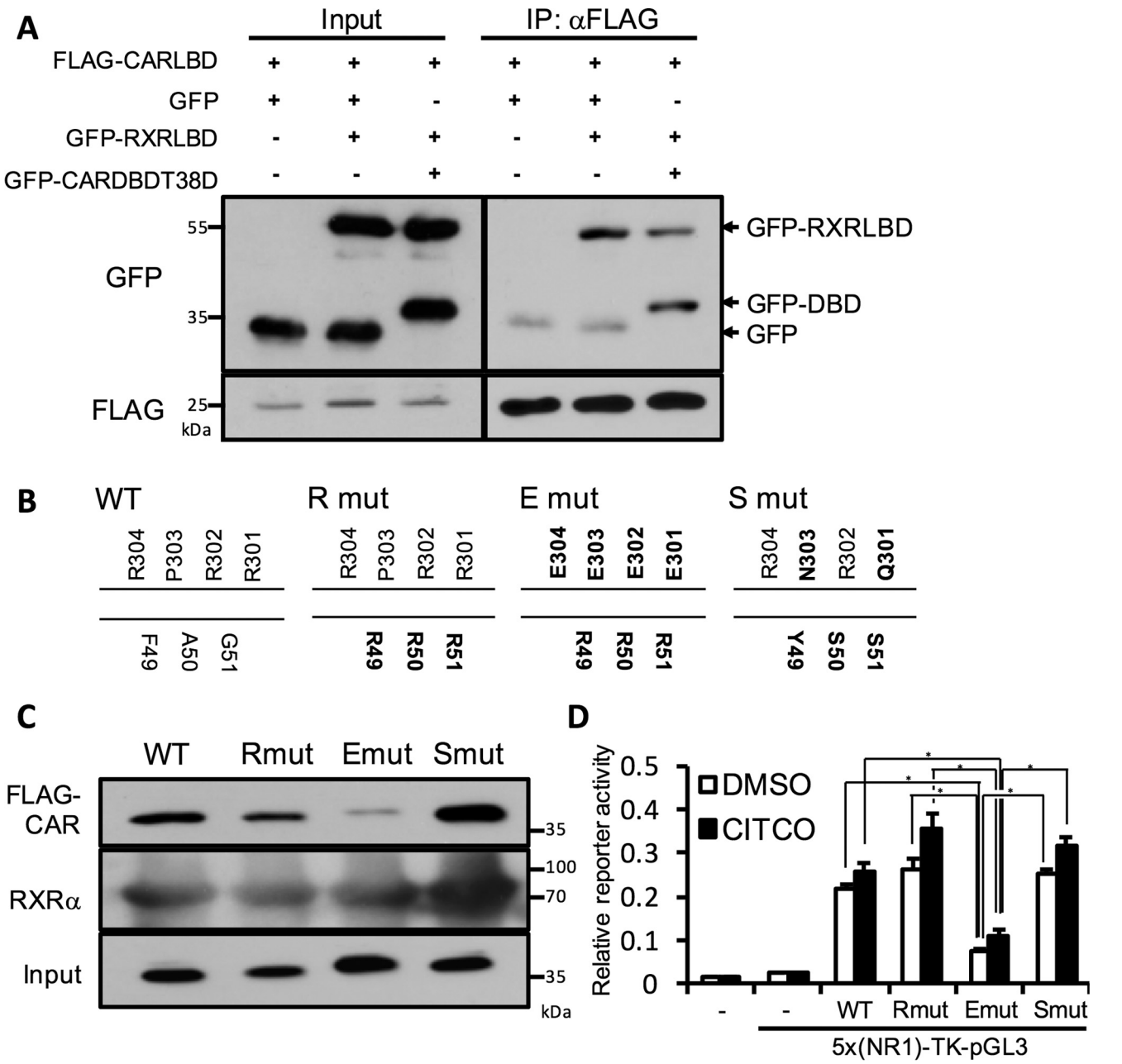

Figure 5. The DBD–LBD interaction regulates CAR heterodimerization with RXRα. *A,* Huh-7 cells were transfected with FLAG–CAR–LBD and GFP–RXRα–LBD in the presence or absence of GFP–DBD–T38D. Cell extracts were immunoprecipitated by an anti-FLAG for subsequent Western blots. *B*, the maps of amino acid sequences and R-, E-, and S-mutations are shown. *C*, pulldown assays. Recombinant HIS–SUMO-tagged RXRα was purified from *E. coli* and immobilized onto Ni-NTA beads and incubated with *in vitro* translated FLAG-tagged CAR-WT, -R mutant (*Rmut*), -E mutant (*Emut*), or -S mutant (*Smut*). Pulled down proteins were subjected to Western blot analysis. *D*, Luc-reporter assays. Huh-7 cells were transfected with 5x(NR1)-TK-pGL3, phRL-TK, and expression plasmids for CAR-WT, -Rmut, -Emut, or -Smut and treated with 0.1% DMSO (*DM*) or CITCO (I, 1 μM) for 24 h. Reporter activities were measured. Values are the mean ± S.D. ($n = 4$). *, $p < 0.05$ (Tukey-Kramer test (GraphPad Prism 6.0 (GraphPad Software)).

action in the presence of DNA oligomers of binding motif TRE (20).

Because recombinant CAR T38D, but not CAR WT, expressed in and purified from *E. coli* cells as its homodimer, phosphorylated CAR's inherent nature may be to homodimerize. However, CAR T38D is primarily expressed as a monomer in Huh-7 cells and homodimerized in response to the EGF signal (10). Thus, there should be a cell signal-mediated regulatory mechanism by which phosphorylated CAR controls this inherent nature. The DBD–LBD interaction takes place between the D-box of the DBD and loop 3 of the LBD as modeled in Fig. 7, *B* and *C*. Loop 3 resides near a previously defined peptide motif (residues from 313 to 319) by the C terminus of CAR LBD, the so-called xenochemical response signal (or XRS) (11). XRS was first defined as a signal peptide that regulates drug-induced nuclear accumulation of CAR in mouse livers (6). Subsequently, XRS was identified as the ERK1/2-binding site of CAR. ERK1/2 was found to bind XRS in response to the EGF signal, homodimerizing phosphorylated CAR to remain inactive (10). Once the EGF signal is repressed by drugs such as PB,

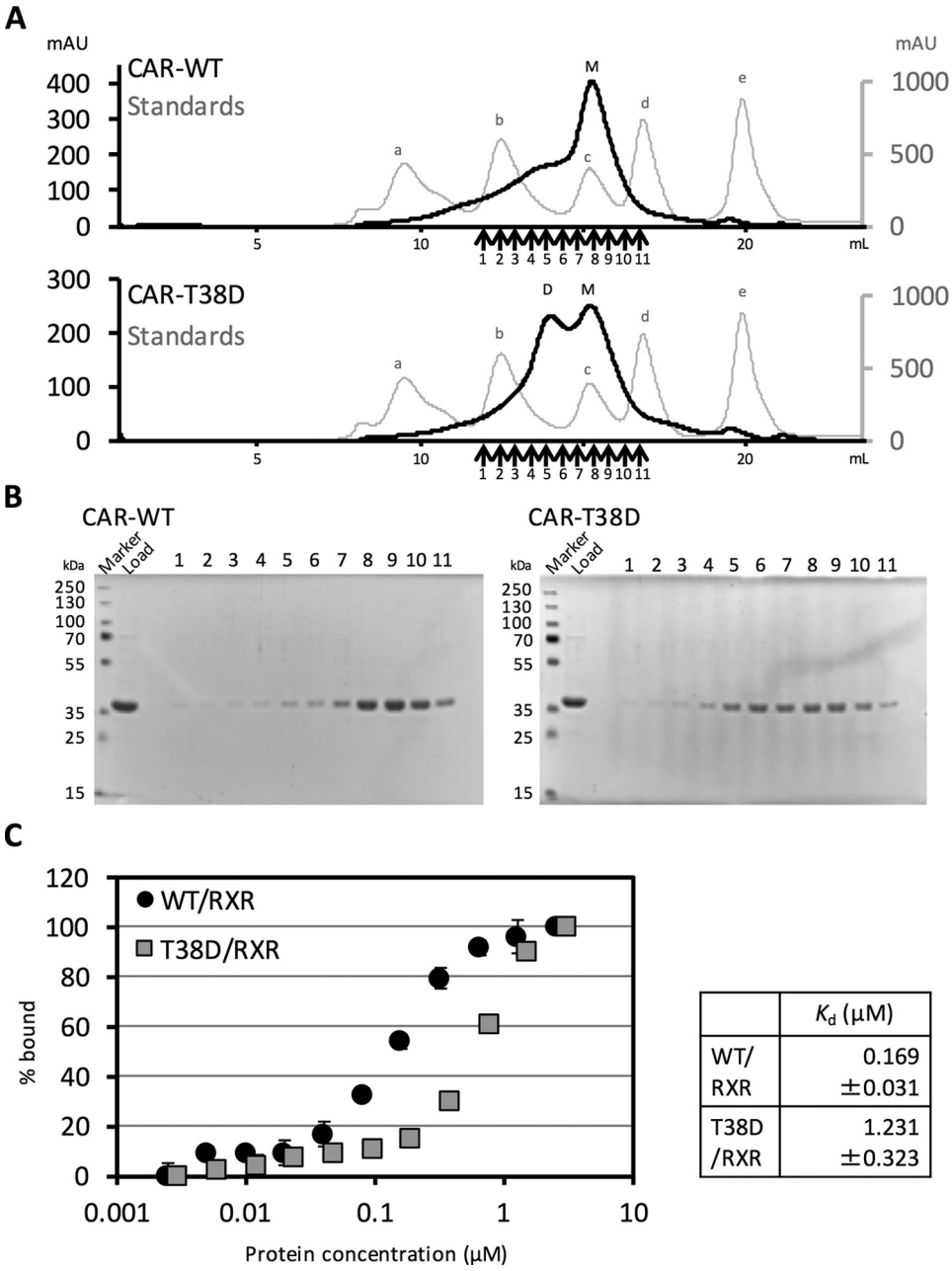

	K_d (μM)
WT/ RXR	0.169 ±0.031
T38D /RXR	1.231 ±0.323

Figure 6. Phosphomimetic mutation at Thr-38 alters oligomerization state and DNA-binding affinity of CAR. *A,* purification and analysis of recombinant human CAR and CAR T38D. CAR proteins were expressed and purified as described under "Experimental procedures." Purified proteins (40 nmol) were subjected to size exclusion chromatography using a Superdex 200 10/300 GL column to assess their molecular sizes. *D*, peaked at 13.9 ml, was considered as CAR dimer (80 kDa); *M*, peaked at 15.2 ml, was considered as a CAR monomer (40 kDa). Elutions of known M_r standards (Gel Filtration Standards (Bio-Rad, number 151–1901) are marked on the plot with *gray*; *a*, thyroglobulin (bovine), 670 kDa, 9.21 ml; *b*, γ-globulin (bovine), 158 kDa, 12.34 ml; *c*, ovalbumin (chicken), 44 kDa, 15.19 ml; *d*, myoglobin (horse), 17 kDa, 16.9 ml; *e*, vitamin B12, 13.5 kDa, 20.1 ml. *B,* fractions indicated by *arrows* in Fig. 5*A* were subjected to SDS-PAGE and stained by Coomassie Brilliant Blue (G-250). *Marker* indicates the protein marker (PageRuler Plus Prestained Protein Ladder (Thermo Fisher Scientific, number 26619)). *Load* indicates the original sample that was loaded into gel filtration. *C,* fluorescent polarization assays. A FAM-labeled NR1 from human *Cyp2b6* promoter was incubated with recombinant CAR WT or CAR T38D with RXRα. After obtaining the data with mP, each mP number was divided with the maximum mP numbers of each protein to calculate the percent of DNA bound relative to the maximum binding of a given protein, and these are shown in the *vertical axis*. Milliporarization (mP) changes over 80 mP in both samples. The *horizontal axis* shows concentrations of CAR proteins. The K_d values were calculated by Kaleidagraph software.

CAR dissociates ERK1/2 and converts to a monomer (3). Therefore, this XRS–ERK1/2 binding may elicit a sort of allosteric effect to CAR extending the hinge, releasing the interaction between D-box and loop 3 interaction, and enabling CAR to form its homodimer.

Our model of CAR conversion also depicts that the hinge extends and the DBD and LBD dissociate allowing active heterodimer with RXRα to form. Upon dephosphorylation of Thr-38, CAR's DBD dissociates from the LBD, extending the hinge to form a heterodimer with RXRα. This CAR–RXRα heterodimer model resembles the recently reported three-dimensional structures of DNA-bound RXRα heterodimers with peroxisome proliferator-activated receptor γ (PPARγ), RAR, and VDR in solution (21–23). In these solution structures, the hinge

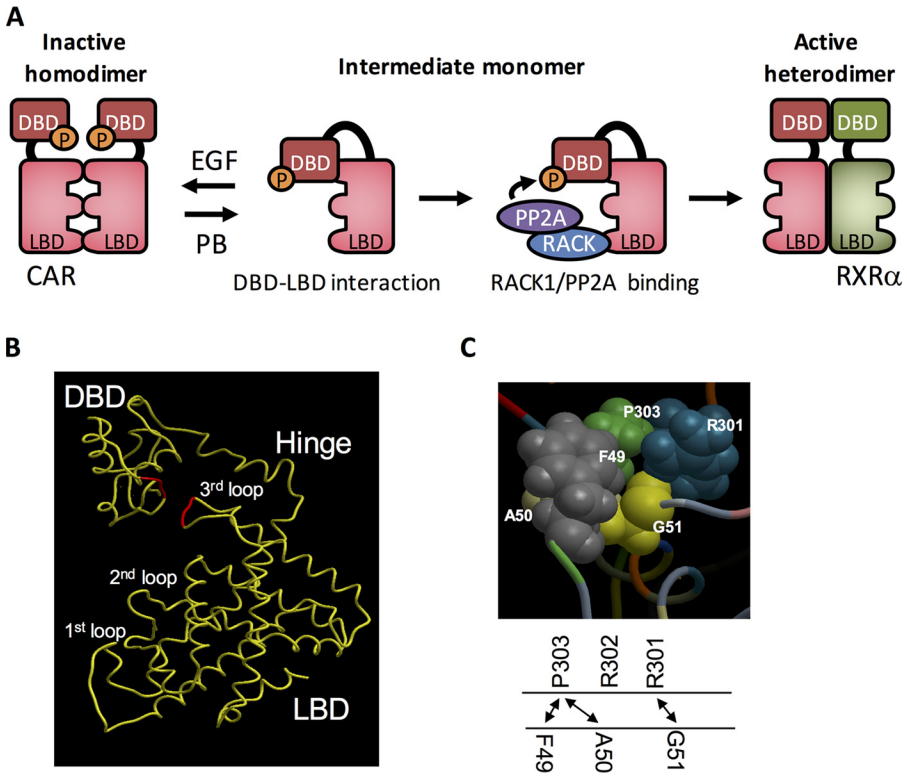

Figure 7. The proposed mode of CAR dimerization. *A,* EGF signal proscribes the DBD interacting with LBD, promoting homodimerization of the phosphorylated CAR monomer. CAR activators such as PB and CITCO dissociate this homodimer back to the monomer, forming a complex with PP2A and RACK1 for dephosphorylation. This dephosphorylated CAR dissociates the DBD from LBD, enabling CAR to heterodimerize with RXRα. *B,* a 3D structure of full-length human CAR. 3D structural model of full-length human CAR was modeled as described under "Experimental procedures" of our previous paper (11). *C,* in this model, the DBD and LBD interact through the D-box of DBD and loop 3 of the LBD.

extends to separate the DBD from LBD so that they do not interact, opening a surface for dimerization. X-ray crystal structures of RXRα heterodimers provide us with a different picture of what a heterodimer should look like (24, 25). In these crystal structures (the DNA-bound PPARγ-RXRα and liver X receptor β (LXRβ)-RXRα heterodimers), the hinge, DBD, and LBD are tightly packed with DNAs in the crystal lattice, in which the DBD interacts with the LBD. Given the caveat that these shrinking hinges and DBD–LBD interactions could forcefully be created during crystallization, the functional significance of these crystal structures remains a critical target of discussion.

CAR homodimerization is regulated through phosphorylation of Thr-38. X-ray crystal structures of the LBD homodimers of GR and androgen receptor revealed that they form homodimers in the absence of DNA utilizing a similar configuration to what we observed with the CAR homodimer (26, 27). The question remains as to how nuclear steroid hormone receptors such as GR and androgen receptor regulate their homodimerization because they do not contain the conserved phosphorylation motif with their DBDs. Although steroid hormone nuclear receptors lack the conserved phosphorylation site within their DBDs, they do contain a long N-terminal domain (NTD) of up to 600 amino acid residues. NTDs of non-steroid nuclear receptors are much shorter in length (*e.g.* only 10 residues for CAR), but they contain conserved phosphorylation sites. It is known that NTDs regulate homodimerization of steroid hormone receptors (14, 19). A role in activation by several potential phosphorylation sites in this region has been proposed (28–30). Despite the differences between these two groups of receptors, both groups appear to utilize the DBD–LBD interaction or the NTD–domains interaction (14, 31, 32) as an underlying structural basis to form homodimers.

In conclusion, the underlying molecular mechanism that regulates CAR activation is its homodimer–monomer–heterodimer conversion; the monomer and homodimer are phosphorylated at Thr-38 and inactive, whereas dephosphorylated CAR can heterodimerize with RXRα to become active. It has now been demonstrated that an intramolecular domain interaction between the DBD and LBD is the determinant regulating this monomer–dimer interaction. Phosphorylation/dephosphorylation of Thr-38 provides CAR with the structural basis that enables CAR to convert between either an inactive monomer or homodimer to a heterodimer with RXRα. In response to the EGF signal, phosphorylated CAR becomes an inactive homodimer. Upon dephosphorylation, the DBD no longer associates with the LBD, allowing the dephosphorylated CAR to form a heterodimer with RXRα. Similar DBD–LBD interactions as those proposed here for CAR are observed in homodimers and heterodimers of various nuclear receptors complexes. Thus, the concept of the DBD–LBD interaction as the underlying principle for CAR activation should be applicable to numerous other nuclear receptors beyond CAR.

Experimental procedures

Reagents

EGF was purchased from Calbiochem; clotrimazole from Selleckchem (Houston, TX); CITCO, anti-FLAG M2 affinity gel (A2220), and horseradish peroxidase (HRP)-conjugated anti-FLAG M2 (S8592) from Sigma; Protein L-agarose (sc-2336), HRP-conjugated antibodies against rabbit IgG (sc-2004), and mouse IgM (sc-2064) from Santa Cruz Biotechnology (Dallas, TX); and antibodies against RACK1 (61078) from BD Biosciences (San Jose, CA); an antibody against GFP (HRP-conjugated) (ab6663) from Abcam (Cambridge, MA); and Ni-NTA-agarose from Qiagen (Valencia, CA).

Plasmids

Human CAR (hCAR) cDNA was previously cloned into pEGFP-c1 (Clontech Laboratories, Palo Alto, CA) (GFP-CAR) (33), was tagged with FLAG at the 5′ end of CAR and cloned into pCR3 (FLAG-CAR) (8). CAR LBD (residues 103–348), CAR DBD (residues 8–76, 8–41, or 42–64), and RXRα LBD (residues 225–462) were cloned into pEGFP-c1 (GFP-CAR LBD, GFP-CAR DBD, and GFP-RXRα LBD, respectively). CAR LBD (residues 103–348) was tagged with FLAG at the N terminus and cloned into pCR3 (FLAG-CAR LBD). 5x(NR1)-TK-pGL3 was previously constructed (34). phRL-TK Control Vector was obtained from Promega. All plasmid constructs and mutations were confirmed by sequencing using PrimeSTAR Max DNA Polymerase (Clontech Laboratories) and proper primers.

Cell cultures

Huh-7 cells were cultured in minimum essential medium (Invitrogen) supplemented with 10% FBS, 2 mM L-glutamine, and 100 units/ml of penicillin/streptomycin. Twenty-four hours after seeding, culture medium was replaced with pre-warmed minimum essential medium without FBS and plasmids were transfected with Lipofectamine 2000 (Invitrogen) according to the manufacturer's instructions. Twenty-four hours after transfection, cells were harvested for subsequent studies.

Co-immunoprecipitations

Co-immunoprecipitation was performed as described previously (10). Whole cell extracts were incubated with FLAG M2-agarose or anti-GFP-agarose at 4 °C overnight. For peptide competition assays, 100 μM peptides of loop 1 (138–147; PAHLFIHHQP), loop 3 (299–308; QQRRPRDRFL) of CAR, or a loop of glucocorticoid receptor (541–557; PEVLYAGYDSSVPDSTW) were incubated with whole cell extracts and anti-FLAG M2 affinity gel overnight. Resultant immune complexes were eluted with SDS-PAGE sample buffer and subjected to Western blot analysis by an antibody as indicated.

SDS-PAGE and Western blot analysis

Protein samples were reduced by 10% β-mercaptoethanol and separated on a 10% SDS-PAGE. Separated proteins were transferred to a polyvinylidene difluoride membrane, which was blocked with TBS containing 5% skim milk and 0.2% Tween 20 and subsequently incubated overnight at 4 °C with primary antibody. After incubating with secondary antibody, proteins were detected by an enhanced chemiluminescence reagent Western Bright ECL (GE Healthcare, Piscataway, NJ). PageRuler Plus Prestained Protein Ladder (Thermo Fisher Scientific, number 26619) was run as a molecular weight marker.

Reporter assays

Huh-7 cells were seeded in a 96-well microplate (Corning Inc., Corning, NY). Twenty-four hours after seeding, cells were transfected with 5x(NR1)-TK-pGL3, phRL-TK, and CAR mutant using Lipofectamine 2000 (Life Technologies) and treated with CITCO (1 μM). Twenty-four hours after transfection, cell lysates were subjected to a Dual Luciferase Assay System (Promega). Firefly luciferase activity was normalized to *Renilla* luciferase activity.

Preparation of recombinant proteins

CAR WT (residues 1–348), CAR T38D (residues 1–348), CAR DBD WT (residues 7–87), CAR DBD T38D (residues 7–87), CAR LBD (residues 103–348), and RXRα (residues 1–462) were expressed as a His_6-SUMO fusion protein. The fusion proteins contain His_6 tag at the N terminus and a ULP-1 cutting site between SUMO and CAR. BL21-CodonPlus (DE3)-RIL (Agilent Technologies, Santa Clara, CA) cells transformed with SUMO-CAR DBD WT/T38D and SUMO-RXRα, and Rosseta2 (DE3) (Novagen, Madison, WI) cells transformed with SUMO-CAR WT/T38D and SUMO-CAR LBD expression plasmids were grown in Terrific broth containing 50 μM clotrimazole at 37 °C to an A_{600} of 0.5–0.7 and induced with 0.2 mM isopropyl 1-thio-β-D-galactopyranoside at 10 °C for 16 h. Cells were collected and resuspended in lysis buffer (25 mM Tris-HCl (pH 7.5), 500 mM NaCl, 1 mM dithiothreitol, 0.35% CHAPS, 100 mM arginine, 100 mM glutamate, 0.1 mM $ZnCl_2$, and 5 μM clotrimazole) and sonicated. The lysate was centrifuged at 38,000 rpm for 45 min, and supernatant was loaded on to a Ni-NTA-agarose column (Qiagen). The column was washed with lysis buffer and eluted with lysis buffer containing 400 mM imidazole. Eluted proteins were cleaved with ULP-1 protease during overnight dialysis with 1000-fold lysis buffer at 4 °C. The His-SUMO and ULP-1 protease was removed by passing through a Ni-NTA-agarose column. The proteins were further purified by gel filtration with Superdex 200 10/300 GL column (GE healthcare) equilibrated with lysis buffer.

Fluorescence polarization assay

Fluorescence polarization experiments were conducted with Polarstar Omega plate reader (BMG Labtech, Durham, NC) using 480 nm excitation and 520 nm emission filters. 20 nM FAM-fluoresceinated NR1 double strands from *CYP2B6* promoter (sense, 5′-FAM labeled, CTGTACTTTCCTGACCCT and antisense, AGGGTCAGGAAAGTACAG) (35) (Integrated DNA Technologies) were mixed with recombinant RXRα and CAR or CAR T38D proteins at various concentrations in a 96-well black polystyrene plate that contains 25 mM Tris-HCl (pH 7.5) buffer containing 100 mM NaCl. The reaction mixture was incubated in 96-well black flat bottom plate (Corning Inc.) for 15 min on ice and data were collected at room temperature.

Calculation of K_d was carried out in Kaleidagraph (Synergy Software, Reading, PA).

In vitro pulldown assays

Recombinant His–SUMO–RXRα was expressed in and purified from BL21-CodonPlus (DE3)-RIL cells and FLAG-CAR mutants were *in vitro* translated using TNT® Quick-coupled Transcription/Translation Systems (Promega). FLAG-CAR mutants were translated by His–SUMO–RXRα and a given CAR mutant was incubated in 25 mM Tris-HCl (pH 7.5) buffer containing 100 mM NaCl, 1 mM dithiothreitol, and Ni-NTA-agarose at 4 °C overnight. After incubation, the Ni-NTA-agarose was washed with the above-mentioned buffer three times, from which pulldown complexes were eluted with SDS-PAGE sample buffer and subjected to Western blot analysis by an antibody as indicated.

Isothermal titration calorimetry

ITC measurements were carried out with SUMO–CAR DBD WT/T38D and CAR LBD in 25 mM Tris-HCl (pH 7.5) buffer containing 100 mM NaCl, 1 mM dithiothreitol, 0.35% CHAPS, 100 mM arginine, 100 mM glutamate, and 5 μM clotrimazole using an iTC$_{200}$ MicroCalorimeter (GE Healthcare) at 25 °C. Substrate solutions containing SUMO–CAR DBD WT/T38D (250 μM) were injected into a reaction cell containing 45 μM CAR LBD. Data acquisition and analysis were performed using the MicroCal Origin software package (Microcal Software, Northhampton, MA). Data analysis was performed by generating a binding isotherm and best fit using the following fitting parameters: n (number of sites), ΔH (cal/mol), ΔS (cal/mol/deg), and K (binding constant in M^{-1}) and the standard Levenberg-Marquardt methods (36). After data analysis, K (M^{-1}) was then converted to K_d (μM).

Author contributions—Conceived and designed the experiments: R. S., J. M., M. S., S. M., L. P., and M. N.; performed the experiments: R. S., J. M., M. S., and S. M.; analyzed the data: R. S., J. M., M. S., L. P., and M. N.; wrote the paper: R. S. and M. N.

Acknowledgments—We thank the Protein Expression Core Facility, NIEHS, for providing anti-GFP-agarose beads for immunoprecipitation and the Mass Spectrometry Core Facility, NIEHS, for conducting mass spectrometry.

References

1. Gao, J., He, J., Zhai, Y., Wada, T., and Xie, W. (2009) The constitutive androstane receptor is an anti-obesity nuclear receptor that improves insulin sensitivity. *J. Biol. Chem.* **284,** 25984–25992 CrossRef Medline
2. Dong, B., Saha, P. K., Huang, W., Chen, W., Abu-Elheiga, L. A., Wakil, S. J., Stevens, R. D., Ilkayeva, O., Newgard, C. B., Chan, L., and Moore, D. D. (2009) Activation of nuclear receptor CAR ameliorates diabetes and fatty liver disease. *Proc. Natl. Acad. Sci. U.S.A.* **106,** 18831–18836 CrossRef Medline
3. Maglich, J. M., Lobe, D. C., and Moore, J. T. (2009) The nuclear receptor CAR (NR1I3) regulates serum triglyceride levels under conditions of metabolic stress. *J. Lipid Res.* **50,** 439–445 CrossRef Medline
4. Sberna, A. L., Assem, M., Gautier, T., Grober, J., Guiu, B., Jeannin, A., Pais de Barros, J. P., Athias, A., Lagrost, L., and Masson, D. (2011) Constitutive androstane receptor activation stimulates faecal bile acid excretion and reverse cholesterol transport in mice. *J. Hepatol.* **55,** 154–161 CrossRef Medline
5. Yamamoto, Y., Moore, R., Goldsworthy, T. L., Negishi, M., and Maronpot, R. R. (2004) The orphan nuclear receptor constitutive active/androstane receptor is essential for liver tumor promotion by phenobarbital in mice. *Cancer Res.* **64,** 7197–7200 CrossRef Medline
6. Dong, B., Lee, J. S., Park, Y. Y., Yang, F., Xu, G., Huang, W., Finegold, M. J., and Moore, D. D. (2015) Activating CAR and β-catenin induces uncontrolled liver growth and tumorigenesis. *Nat. Commun.* **6,** 5944 CrossRef Medline
7. Mutoh, S., Sobhany, M., Moore, R., Perera, L., Pedersen, L., Sueyoshi, T., and Negishi, M. (2013) Phenobarbital indirectly activates the constitutive active androstane receptor (CAR) by inhibition of epidermal growth factor receptor signaling. *Sci. Signal.* **6,** ra31 Medline
8. Osabe, M., and Negishi, M. (2011) Active ERK1/2 protein interacts with the phosphorylated nuclear constitutive active/androstane receptor (CAR; NR1I3), repressing dephosphorylation and sequestering CAR in the cytoplasm. *J. Biol. Chem.* **286,** 35763–35769 CrossRef Medline
9. Yasujima, T., Saito, K., Moore, R., and Negishi, M. (2016) Phenobarbital and insulin reciprocate activation of the nuclear receptor constitutive androstane receptor through the insulin receptor. *J. Pharmacol. Exp. Ther.* **357,** 367–374 CrossRef Medline
10. Shizu, R., Osabe, M., Perera, L., Moore, R., Sueyoshi, T., and Negishi, M. (2017) Phosphorylated nuclear receptor CAR forms a homodimer to repress its constitutive activity for ligand activation. *Mol. Cell. Biol.* **37,** e00649 Medline
11. Mutoh, S., Osabe, M., Inoue, K., Moore, R., Pedersen, L., Perera, L., Rebolloso, Y., Sueyoshi, T., and Negishi, M. (2009) Dephosphorylation of threonine 38 is required for nuclear translocation and activation of human xenobiotic receptor CAR (NR1I3). *J. Biol. Chem.* **284,** 34785–34792 CrossRef Medline
12. Dahlman-Wright, K., Wright, A., Gustafsson, J. A., and Carlstedt-Duke, J. (1991) Interaction of the glucocorticoid receptor DNA-binding domain with DNA as a dimer is mediated by a short segment of five amino acids. *J. Biol. Chem.* **266,** 3107–3112 Medline
13. Luisi, B. F., Xu, W. X., Otwinowski, Z., Freedman, L. P., Yamamoto, K. R., and Sigler, P. B. (1991) Crystallographic analysis of the interaction of the glucocorticoid receptor with DNA. *Nature* **352,** 497–505 CrossRef Medline
14. van Royen, M. E., van Cappellen, W. A., de Vos, C., Houtsmuller, A. B., and Trapman, J. (2012) Stepwise androgen receptor dimerization. *J. Cell Sci.* **125,** 1970–1979 CrossRef Medline
15. Honkakoski, P., Zelko, I., Sueyoshi, T., and Negishi, M. (1998) The nuclear orphan receptor CAR-retinoid X receptor heterodimer activates the phenobarbital-responsive enhancer module of the CYP2B gene. *Mol. Cell. Biol.* **18,** 5652–5658 CrossRef Medline
16. Koike, C., Moore, R., and Negishi, M. (2007) Extracellular signal-regulated kinase is an endogenous signal retaining the nuclear constitutive active/androstane receptor (CAR) in the cytoplasm of mouse primary hepatocytes. *Mol. Pharmacol.* **71,** 1217–1221 CrossRef Medline
17. Kanno, Y., Suzuki, M., Nakahama, T., and Inouye, Y. (2005) Characterization of nuclear localization signals and cytoplasmic retention region in the nuclear receptor CAR. *Biochim. Biophys. Acta* **1745,** 215–222 CrossRef Medline
18. Savory, J. G., Préfontaine, G. G., Lamprecht, C., Liao, M., Walther, R. F., Lefebvre, Y. A., and Haché, R. J. (2001) Glucocorticoid receptor homodimers and glucocorticoid-mineralocorticoid receptor heterodimers form in the cytoplasm through alternative dimerization interfaces. *Mol. Cell. Biol.* **21,** 781–793 CrossRef Medline
19. Tetel, M. J., Jung, S., Carbajo, P., Ladtkow, T., Skafar, D. F., and Edwards, D. P. (1997) Hinge and amino-terminal sequences contribute to solution dimerization of human progesterone receptor. *Mol. Endocrinol.* **11,** 1114–1128 CrossRef Medline
20. Putcha, B. D., and Fernandez, E. J. (2009) Direct interdomain interactions can mediate allosterism in the thyroid receptor. *J. Biol. Chem.* **284,** 22517–22524 CrossRef Medline

21. Orlov, I., Rochel, N., Moras, D., and Klaholz, B. P. (2012) Structure of the full human RXR/VDR nuclear receptor heterodimer complex with its DR3 target DNA. *EMBO J.* **31,** 291–300 CrossRef Medline
22. Rochel, N., Ciesielski, F., Godet, J., Moman, E., Roessle, M., Peluso-Iltis, C., Moulin, M., Haertlein, M., Callow, P., Mély, Y., Svergun, D. I., and Moras, D. (2011) Common architecture of nuclear receptor heterodimers on DNA direct repeat elements with different spacings. *Nat. Struct. Mol. Biol.* **18,** 564–570 CrossRef Medline
23. Helsen, C., and Claessens, F. (2014) Looking at nuclear receptors from a new angle. *Mol. Cell. Endocrinol.* **382,** 97–106 CrossRef Medline
24. Chandra, V., Huang, P., Hamuro, Y., Raghuram, S., Wang, Y., Burris, T. P., and Rastinejad, F. (2008) Structure of the intact PPAR-γ-RXR-nuclear receptor complex on DNA. *Nature* **456,** 350–356 Medline
25. Lou, X., Toresson, G., Benod, C., Suh, J. H., Philips, K. J., Webb, P., and Gustafsson, J. A. (2014) Structure of the retinoid X receptor α-liver X receptor β (RXRα-LXRβ) heterodimer on DNA. *Nat. Struct. Mol. Biol.* **21,** 277–281 CrossRef Medline
26. Bledsoe, R. K., Montana, V. G., Stanley, T. B., Delves, C. J., Apolito, C. J., McKee, D. D., Consler, T. G., Parks, D. J., Stewart, E. L., Willson, T. M., Lambert, M. H., Moore, J. T., Pearce, K. H., and Xu, H. E. (2002) Crystal structure of the glucocorticoid receptor ligand binding domain reveals a novel mode of receptor dimerization and coactivator recognition. *Cell* **110,** 93–105 CrossRef Medline
27. Nadal, M., Prekovic, S., Gallastegui, N., Helsen, C., Abella, M., Zielinska, K., Gay, M., Vilaseca, M., Taulès, M., Houtsmuller, A. B., van Royen, M. E., Claessens, F., Fuentes-Prior, P., and Estèbanez-Perpina, E. (2017) Structure of the homodimeric androgen receptor ligand-binding domain. *Nat. Commun.* **8,** 14388 CrossRef Medline
28. Chen, S., Xu, Y., Yuan, X., Bubley, G. J., and Balk, S. P. (2006) Androgen receptor phosphorylation and stabilization in prostate cancer by cyclin-dependent kinase 1. *Proc. Natl. Acad. Sci. U.S.A.* **103,** 15969–15974 CrossRef Medline
29. Guo, Z., Dai, B., Jiang, T., Xu, K., Xie, Y., Kim, O., Nesheiwat, I., Kong, X., Melamed, J., Handratta, V. D., Njar, V. C., Brodie, A. M., Yu, L. R., Veenstra, T. D., Chen, H., and Qiu, Y. (2006) Regulation of androgen receptor activity by tyrosine phosphorylation. *Cancer Cell* **10,** 309–319 CrossRef Medline
30. Grimm, S. L., Hartig, S. M., and Edwards, D. P. (2016) Progesterone receptor signaling mechanisms. *J. Mol. Biol.* **428,** 3831–3849 CrossRef Medline
31. Kraus, W. L., McInerney, E. M., and Katzenellenbogen, B. S. (1995) Ligand-dependent, transcriptionally productive association of the amino- and carboxyl-terminal regions of a steroid hormone nuclear receptor. *Proc. Natl. Acad. Sci. U.S.A.* **92,** 12314–12318 CrossRef Medline
32. Takimoto, G. S., Tung, L., Abdel-Hafiz, H., Abel, M. G., Sartorius, C. A., Richer, J. K., Jacobsen, B. M., Bain, D. L., and Horwitz, K. B. (2003) Functional properties of the N-terminal region of progesterone receptors and their mechanistic relationship to structure. *J. Steroid Biochem. Mol. Biol.* **85,** 209–219 CrossRef Medline
33. Zelko, I., Sueyoshi, T., Kawamoto, T., Moore, R., and Negishi, M. (2001) The peptide near the C terminus regulates receptor CAR nuclear translocation induced by xenochemicals in mouse liver. *Mol. Cell. Biol.* **21,** 2838–2846 CrossRef Medline
34. Kawamoto, T., Sueyoshi, T., Zelko, I., Moore, R., Washburn, K., and Negishi, M. (1999) Phenobarbital-responsive nuclear translocation of the receptor CAR in induction of the CYP2B gene. *Mol. Cell. Biol.* **19,** 6318–6322 CrossRef Medline
35. Sueyoshi, T., Kawamoto, T., Zelko, I., Honkakoski, P., and Negishi, M. (1999) The repressed nuclear receptor CAR responds to phenobarbital in activating the human CYP2B6 gene. *J. Biol. Chem.* **274,** 6043–6046 CrossRef Medline
36. Sobhany, M., Kakuta, Y., Sugiura, N., Kimata, K., and Negishi, M. (2012) The structural basis for a coordinated reaction catalyzed by a bifunctional glycosyltransferase in chondroitin biosynthesis. *J. Biol. Chem.* **287,** 36022–36028 CrossRef Medline